

Crystal Structure of Silver Pentazolates AgN_5 and AgN_6

Ashley S. Williams, Kien Nguyen Cong, Joseph M. Gonzalez, and Ivan I.
Oleynik*

Department of Physics, University of South Florida, Tampa, FL 33620

E-mail: oleynik@usf.edu

Abstract

Silver pentazolate, a high energy density compound containing cyclo- N_5^- anion, has recently been synthesized at ambient conditions. However, due to high sensitivity to irradiation, its crystal structure has not been determined. In this work, silver-nitrogen crystalline compounds at ambient conditions and high pressures, up to 100 GPa, are predicted and characterized by performing first-principles evolutionary crystal structure searching with variable stoichiometry. It is found that newly discovered AgN_5 and AgN_6 are the only thermodynamically stable silver-nitrogen compounds at pressures between 42 and 80 GPa. In contrast to AgN_5 , pentazolate AgN_6 compound contains N_2 diatomic molecules in addition to cyclo- N_5^- . These AgN_5 and AgN_6 crystals are metastable at ambient conditions with positive formation enthalpies of 54.95 kJ/mol and 46.24 kJ/mol, respectively. The underlying cause of the stability of cyclo- N_5^- silver pentazolates is the enhanced aromaticity enabled by the charge transfer from silver atoms to nitrogen rings. To aid in experimental identification of these materials, calculated Raman spectra are reported at ambient pressure: the frequencies of N_5^- vibrational modes of AgN_5 are in good agreement with those measured in experiment.

Introduction

Polynitrogen high energy density materials are in the focus of intense experimental and theoretical investigations^{1,2} due to their promise of delivering high explosive power upon decomposition of single and double bonded nitrogen atoms to triply bonded N_2 ^{3,4}. Although pure nitrogen extended solids such as cubic gauche (cg) and layered polymeric nitrogen have been predicted⁵ and subsequently synthesized at high pressures^{6,7}, their recovery at ambient conditions is challenging⁸.

Another possibility to achieve high energy density is to realize compounds containing single and double bonded nitrogen molecular species, such as cyclo- N_5^- anion.⁹⁻¹⁸ The negative charge on pentazoles requires an electron donating component, therefore, a family of alkali pentazolate crystals have been predicted^{10-13,19-23} and then synthesized^{9,12,14-18,24,25} at high pressures. Success has recently been achieved in synthesizing cyclo- N_5^- pentazolates at ambient conditions using traditional methods of synthetic chemistry^{9,14-17}. However, the challenge of recovering simpler cyclo- N_5^- pentazolate compounds at ambient conditions still remains.

Most of metal pentazolates discovered so far are the crystals with alkali cations Li^+ ^{18,21,23,24}, Na^+ ^{10,25}, K^+ ¹⁹, and Rb^+ ¹³ with 1:5 metal/nitrogen stoichiometry. They are just the one of several M_xN_y materials featuring isolated nitrogen atoms/ions, finite and infinite chains, 2D layers and other polynitrogen complexes. Such rich chemistry is due to the ease of alkali atoms to donate electrons to nitrogen species, resulting in plethora of M_xN_y chemical compositions.

Silver, being one of the coinage elements (Cu, Ag, and Au), is “noble”, i.e. almost unreactive, compared to reactive alkali metals. This is because the outer valence electrons are more tightly bound than those of alkali atoms due to poor screening of the nuclear charge by the d- sub-shells compared to much stronger screening by filled s/p shells of alkali atoms. Therefore, less variety is expected among stoichiometries of Ag_xN_y compounds; it is highly probable that 1:5 stoichiometry would be the only one that displays negative formation

enthalpies at high pressures. In fact, even the existence of AgN_5 was questioned more than a century ago when it was purportedly synthesized by Lifschitz²⁶ and then refuted by Curtius *et al.*²⁷. Only two silver nitrogen crystalline compounds are known to exist at ambient conditions: silver nitride Ag_3N ²⁸ and silver azide AgN_3 ²⁹, both of them being extremely sensitive explosive materials³⁰⁻³².

Sun et al. reported the synthesis of a solvent-free pentazolate complex AgN_5 in a compound which does not contain counter ions such as Cl^- , NH_4^+ and H_3O^+ ¹⁷. The authors failed to obtain single crystal AgN_5 suitable to XRD characterization as this compound is highly unstable upon irradiation or heating. Instead, they converted AgN_5 complex to a 3D framework $[\text{Ag}(\text{NH}_3)_2]^+[\text{Ag}_3(\text{N}_5)_4]^-$ in order to characterize its crystal structure. Therefore, the important question is whether AgN_5 exists and if it does, what is its crystal structure. The light and heat instability of AgN_5 indicates a high degree of its metastability, similar to known silver azide AgN_3 crystal which possesses a very high positive enthalpy of formation 310.3 kJ/mol³³.

It is known that application of pressure imparts a substantial thermomechanical energy of compression to precursor materials³⁴, which may promote unusual chemistry of resulting compounds. Therefore, the investigation of AgN_5 as well as other Ag-N materials with different stoichiometries (if they exist) at high pressures is of great importance for elucidating bonding and structure of silver-nitrogen compounds.

The goal of this research is to answer these outstanding questions by performing crystal structure searching of new silver-nitrogen crystalline compounds, including AgN_5 , at ambient conditions and high pressures up to 100 GPa using variable composition first-principles evolutionary crystal structure prediction method. Once the new compounds are uncovered their stability, bonding and structure as well as electronic and vibrational properties are analyzed. Chemical pathways for synthesis of discovered thermodynamically stable compounds are proposed and Raman spectra of the resultant compounds are calculated to aid in experimental detection of these materials at ambient pressure.

Computational Details

The silver-nitrogen compounds Ag_xN_y of variable stoichiometry are searched using first-principles evolutionary structure prediction method implemented in Universal Structure Predictor: Evolutionary Xtallography code (USPEX)³⁵⁻³⁷. The variable composition searches are performed at several pressures using unit cells containing varying amounts of silver and nitrogen atoms between 8 to 16 atoms in the cell. In total, about 100 different Ag_xN_y stoichiometries are sampled. Once the variable composition search at a given pressure is complete, fixed composition or molecular searches using larger unit cell sizes up to 48 atoms are performed at stoichiometries corresponding to the thermodynamically stable compounds at the vertices of the convex hull and the metastable compounds up to 20 meV above the convex hull.

The process of structure prediction begins by generating structures based on all space groups and random lattice parameters in the first generation. The obtained structures are then optimized to a target pressure. Their normalized formation enthalpy is determined as follows:

$$\Delta H_{\text{Ag}_x\text{N}_y} = (H_{\text{Ag}_x\text{N}_y} - xH_{\text{Ag}} - yH_{\text{N}})/(x + y),$$

where $H_{\text{Ag}_x\text{N}_y}$, H_{Ag} and H_{N} are enthalpy of the compounds and best structures of pure elements, respectively. Based on the normalized formation enthalpy, the convex hull at each pressure is constructed using the lowest formation enthalpy structures. For each subsequent generation, a small subset of the lowest enthalpy structures is kept while a new generation is built by adding more random crystals and by applying variation operators to the best “parent” structures. The process is repeated until the best kept structures do not change for ten consecutive generations.

Once combined variable and fixed stoichiometry searches are completed at several pressures, all the resulting crystal structures are combined in one single database, which is then

used for high precision geometry optimization and construction of the final convex hull at every pressure of our interest, from 0 to 100 GPa. Such combined method was shown to be successful in overcoming computational limitations of the variable composition search. For example, during variable composition search at 50 GPa only one thermodynamically stable stoichiometry, AgN_5 , was found. However, a second thermodynamically stable stoichiometry AgN_6 was uncovered in subsequent fixed stoichiometry molecular search using twice larger unit cell containing four silver atoms and twenty-four nitrogen atoms.

The USPEX method and similar structure search methods^{38,39} have already been successful in prediction of experimentally known crystal structures of pure elements. To speed up the search, the known lowest enthalpy reference structures of pure elements were taken: fcc Ag-*Fm-3m* for Ag across the entire pressure range, and $\alpha\text{-N}_2$ at 0 GPa, $\varepsilon\text{-N}_2$ at 50 GPa, and cg-N above 50 GPa for reference structures of nitrogen. If a compound lies on the convex hull it is considered thermodynamically stable meaning it will not decompose into either the pure elements or into a mixture of other Ag_xN_y compounds⁴⁰. Compounds that lie above the convex hull must be dynamically stable, i.e. no negative phonon frequencies, to be considered metastable.

Perdew-Burke-Ernzerhof (PBE) generalized gradient approximation (GGA) to DFT⁴¹ implemented in Vienna ab initio simulation package VASP⁴² is used to perform the first-principles calculations. The projector augmented wave (PAW) pseudopotentials are employed. During the USPEX search, each crystal is optimized using a plane wave basis set with 500 eV energy cutoff and k-point sampling density of 0.07 \AA^{-1} . At the completion of a search, the structures that are on the convex hull as well as a subset of possible metastable structures with higher formation energy, up to 100 meV above the convex hull, are optimized using high accuracy setting to generate the accurate convex hull. During the high accuracy calculations, the hard nitrogen PAW pseudopotential is used to address a possibility of overlapping cores of N atoms in triple bonded N_2 . In addition, the energy cutoff and k-point density are increased to 1000 eV and 0.03 \AA^{-1} respectively. Frozen phonon approximation is

used to calculate the phonons at the gamma point as well as off-resonant Raman frequencies.⁴³ The intensities are determined by calculating the macroscopic dielectric polarizability tensors for each normal mode eigenvector.⁴⁴ The atomic charges and bond orders are calculated using density derived electrostatic and chemical charges (DDEC) method implemented in VASP.⁴⁵

Results and discussion

At 0 GPa, no negative formation enthalpy Ag_xN_y compounds exist, therefore, a concave hull consists of metastable structures with positive formation enthalpies. This is in agreement with the fact that at ambient conditions only two known silver-nitrogen compounds, silver nitride (Ag_3N) and silver azide (AgN_3), possess very high positive formation enthalpies.

At 50 GPa, the stoichiometries with negative formation enthalpy are thermodynamically stable AgN_5 , and AgN_6 , and metastable AgN_9 , and AgN_4 , see the convex hull in Fig. 1. At 60 GPa and 70 GPa only $\text{AgN}_5\text{-}P2_1/c$ is on the convex hull while $\text{AgN}_6\text{-}P2_12_12$ becomes metastable with 1.93 meV/atom and 17.4 meV/atom above the convex hull at each pressure respectively.

Both $\text{AgN}_5\text{-}P2_1/c$ and $\text{AgN}_6\text{-}P2_12_12$ follow the pattern of NaN_5 which contains a single phase of XN_5 over the entire pressure range¹⁰ whereas KN_5 , RbN_5 , and CsN_5 consist of a low pressure and a high pressure phases.^{10,11,13,19} The formation enthalpy of $\text{AgN}_5\text{-}P2_1/c$ becomes negative for the first time at 41.5 GPa. At 57.5 GPa, $\text{AgN}_5\text{-}P2_1/c$ reaches its lowest formation enthalpy of -0.095 eV/atom. Finally, at 79.4 GPa, the formation enthalpy of $\text{AgN}_5\text{-}P2_1/c$ becomes positive again. Similarly, the formation enthalpy of $\text{AgN}_6\text{-}P2_12_12$ becomes negative at 41.7 GPa. At 57.5 GPa, the formation enthalpy $\text{AgN}_6\text{-}P2_12_12$ reaches the lowest value of -0.086 eV/atom. The formation enthalpy of $\text{AgN}_6\text{-}P2_12_12$ becomes positive again at pressures exceeding 68 GPa.

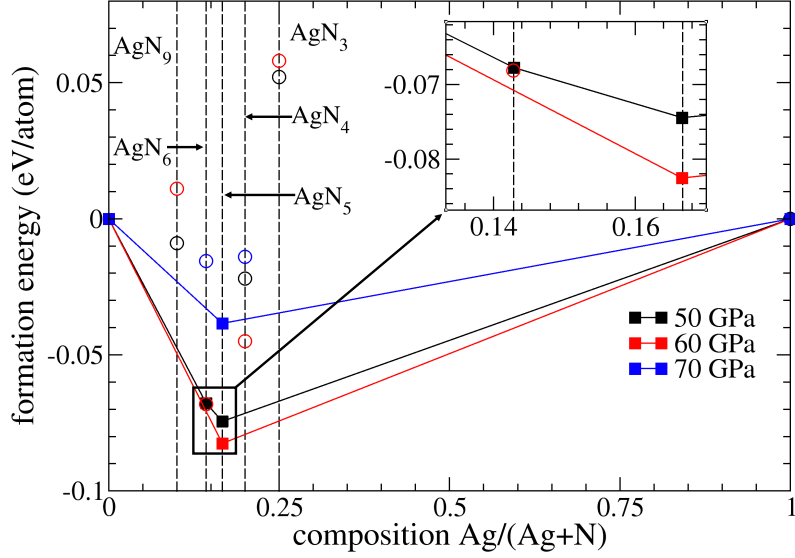


Figure 1: Ag-N convex hulls at 50, 60, and 70 GPa. Filled squares indicate thermodynamically stable structures; open circles – metastable structures.

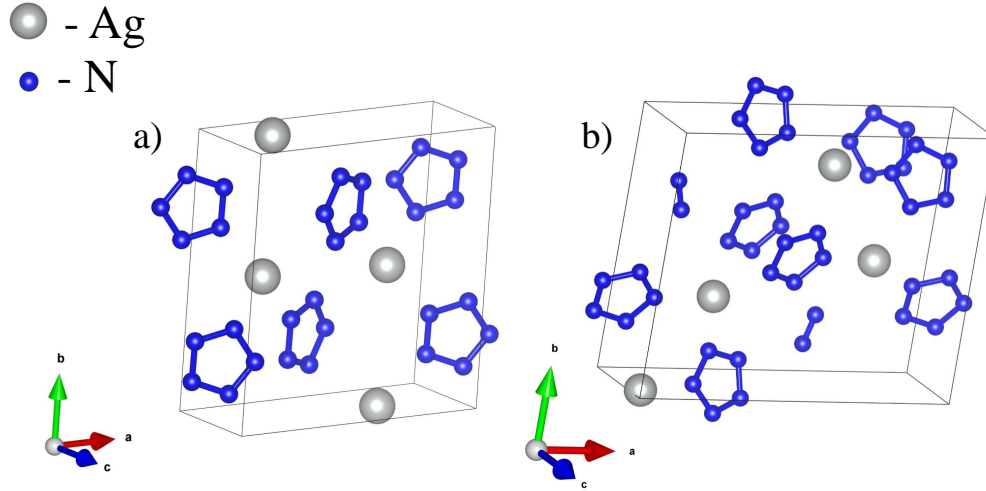


Figure 2: Crystal structure of a) $\text{AgN}_5\text{-}P2_1/c$ and b) $\text{AgN}_6\text{-}P2_12_12$ pentazolates. The Ag atoms are depicted in gray and the N atoms are depicted in blue.

The crystal structures of the two new compounds are depicted in Fig. 2. There are 24 atoms in the $\text{AgN}_5\text{-}P2_1/c$ unit cell and 28 atoms in the $\text{AgN}_6\text{-}P2_12_12$ unit cell. In $\text{AgN}_5\text{-}P2_1/c$, nitrogen atoms form 5 membered cyclo- N_5^- pentazolate rings with the silver atoms not covalently bonded to the nitrogen rings or other silver atoms. The packing efficiency of $\text{AgN}_5\text{-}$

$P2_1/c$ is 43.8%. The distance between the molecular centers of nearest neighboring cyclo- N_5^- pentazolate rings in AgN_5-P2_1/c is approximately 5 Å. In $AgN_6-P2_12_12$, nitrogen atoms form cyclo- N_5^- with extra, isolated N_2 dimers and standalone silver atoms. The packing efficiency of $AgN_6-P2_12_12$ is 24.6%. The molecular centers of nearest neighboring cyclo- N_5^- pentazolate rings in $AgN_6-P2_12_12$ are separated by approximately 5.2 Å. The cyclo- N_5^- pentazolate rings of both AgN_5-P2_1/c and $AgN_6-P2_12_12$ are isolated with bonding only occurring between the nitrogen atoms within each individual ring. The electronic band structure of both predicted silver pentazolate crystals display insulator character at all pressures studied, see Figs. S1 and S2 in the supplementary information.

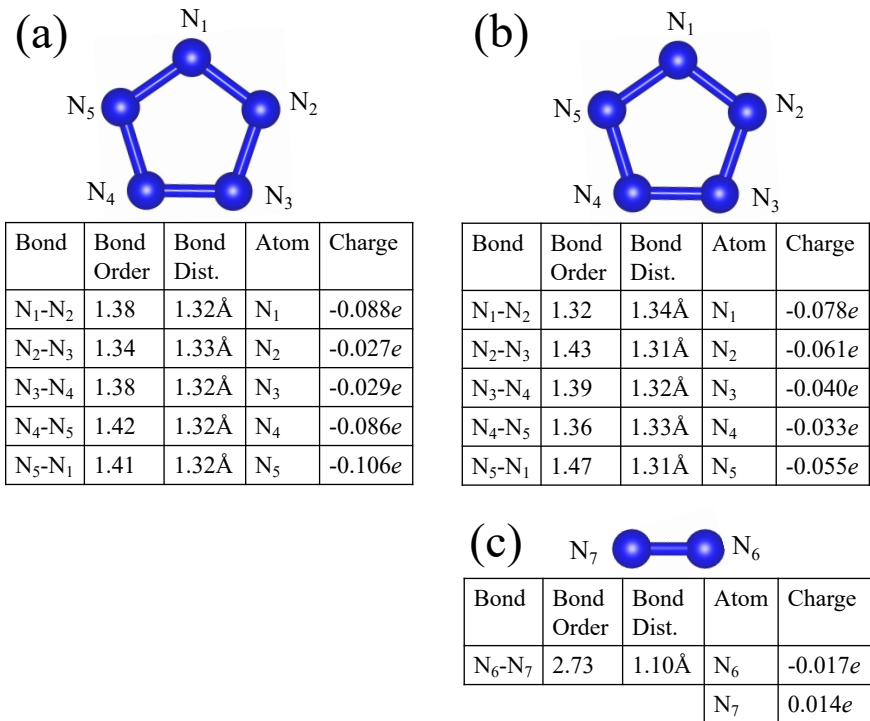


Figure 3: a) The charges and bond order in the cyclo- N_5^- pentazolate in the AgN_5-P2_1/c crystal. The N-N bond lengths in cyclo- N_5^- pentazolate between each silver atom is between 1.33 Å and 1.33 Å. b) The charges and bond order in the cyclo- N_5^- pentazolate in the $AgN_6-P2_12_12$ crystal. The N-N bond lengths in the cyclo- N_5^- pentazolate is between 1.31 and 1.34 Å. c) The charges and bond order in the N_2 dimer in the $AgN_6-P2_12_12$ crystal: the N-N bond length is 1.10 Å.

To understand the bonding of these novel compounds, the charges and bond orders were calculated, see Fig. 3. The N-N bond lengths in the pentazolate cyclo-N₅⁻ anions in AgN₅-P2₁/c are between 1.32 Å and 1.33 Å. The charges, beginning from the atom at the top point of the pentazolate ring shown in Fig. 3(a) and moving clockwise, are: -0.088e, -0.027e, -0.029e, -0.086e, and -0.106e. The silver atom carries charge +0.33e, the corresponding negative charge is on N₅⁻ anion. The aromatic nature of the cyclo-N₅⁻ can be deduced from the N-N bond orders which range from 1.34 to 1.42, i.e. between those corresponding to single and double bonds. The average charge and average N-N bond order in the cyclo-N₅⁻ in AgN₅-P2₁/c are similar to their counterparts in the cyclo-N₅⁻ in XN₅ {X = Na, K, Rb, Cs} compounds.^{10,11,13,19}

The N-N bond lengths in cyclo-N₅⁻ in AgN₆-P2₁2₁2 crystal are between 1.31 and 1.34 Å which are slightly smaller than those of its pure pentazolate counterpart, AgN₅-P2₁/c. As seen in Fig. 3(b), the charges on the nitrogen atoms in the AgN₆-P2₁2₁2 pentazolate are also smaller on average than those in AgN₅-P2₁/c crystal, ranging from -0.033e to -0.078e. The N₂ dimer of AgN₆-P2₁2₁2 is almost electroneutral, as the atomic charges on N atoms -0.017e and 0.014e compensate each other, see Fig. 3c. The silver atoms in AgN₆-P2₁2₁2 carry a charge of 0.27e. Though the charges are smaller in AgN₆-P2₁2₁2 crystal than in AgN₅-P2₁/c, the N-N bond orders are comparable, ranging from 1.32 to 1.47 in case of AgN₆-P2₁2₁2. The N-N bond of the N₂ dimer in AgN₆-P2₁2₁2 is close to a triple bond in isolated diatomic N₂ molecule with N-N bond length 1.1 Å and bond order 2.73.

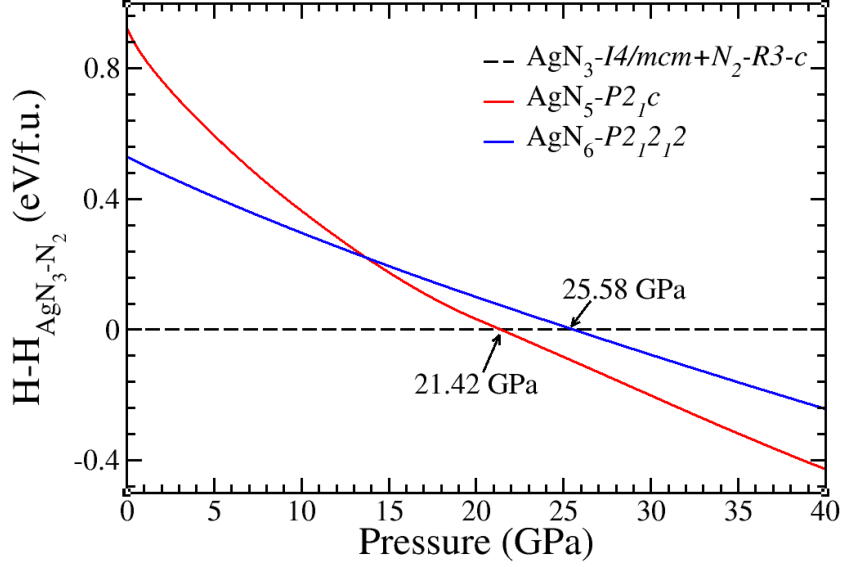


Figure 4: Enthalpy difference as a function of pressure between $\text{AgN}_5\text{-}P2_1/c$ (red) and $\text{AgN}_6\text{-}P2_12_12$ (blue) and a mixture of possible precursors, silver azide AgN_3 and nitrogen N_2 .

In principle, the new compounds can be synthesized via compression of silver azide and nitrogen in a diamond anvil cell (DAC). Several attempts have been made to produce pentazolate salts via traditional DAC experiments whereby a combination of a metal azide and molecular nitrogen is cold compressed to high pressures and then laser heated. CsN_5 was synthesized, having first been guided by first-principles crystal structure prediction, by Steele *et al.*¹¹ via compression of $\text{CsN}_5 + \text{N}_2$ in DAC to 60 GPa. Zhou *et al.*²⁴ compressed lithium azide and molecular nitrogen in DAC to pressure of only 41.1 GPa and report the formation of a new phase of $\text{LiN}_5\text{-}P2_1/m$. Zhou *et al.*'s results are consistent with predictions of the transition pressure of 40 GPa by Yi *et al.*²³ and Peng *et al.*²². Recently, the formation of two new pentazolate salts, NaN_5 and $\text{NaN}_5\cdot\text{N}_2$, were observed via DAC experiments of sodium azide and molecular nitrogen compressed to ~ 50 GPa.²⁵ Notably, the $\text{NaN}_5\cdot\text{N}_2$ crystal synthesized by Bykov *et al.* contains both cyclo- N_5^- pentazolate rings and N_2 dimers similar to what is predicted here for $\text{AgN}_6\text{-}P2_12_12$.

Silver azide, in spite of its volatility, is well studied with a known phase transition from low pressure $\text{AgN}_3\text{-}Ibam$ to high pressure $\text{AgN}_3\text{-}I4/mcm$ at 2.7 GPa.^{46,47} The theoretical study presented by W. Zhu *et al.* predicts this transition to occur at nearly 7 GPa⁴⁸ how-

ever, our results are closer to what was found in experiments with AgN_3 - $I4/mcm$ becoming energetically favorable near 1.5 GPa.

The enthalpy difference between AgN_5 - $P2_1/c$ and AgN_6 - $P2_12_12$ and the possible precursors, AgN_3 - $I4/mcm$ and N_2 - $R3-c$, was calculated over increasing pressure as a zero-temperature estimate of potential transformation of the precursors to the pentazolate product, see Fig. 4. AgN_3 - $I4/mcm$ is taken as the precursor due to the phase transition from AgN_3 - $Ibam$ to AgN_3 - $I4/mcm$ that occurs at such a low pressure. The results show that AgN_5 - $P2_1/c$ and AgN_6 - $P2_12_12$ are thermodynamically favorable to the mixture of the precursors at 0 K and pressures exceeding 21 GPa and 26 GPa respectively.

It is important to note that 0 K data are the lowest pressure estimates. The transition pressures at high temperatures are determined by a complex interplay of thermodynamics and kinetics of solid-state reactions.⁴⁹ On the one hand, temperature helps to activate kinetics, thus potentially lowering transition pressure.⁵⁰ On the other hand, temperature might thermodynamically stabilize the molecular precursors compared to solid reactants due to entropic $-TS$ contribution to the Gibbs free energy, thus increasing transition pressure upon increase of temperature.^{49,51} Due to extreme complexity of the phenomena involved a meaningful predictions of finite temperature effects seem to be impractical to make within the scope of the current work.

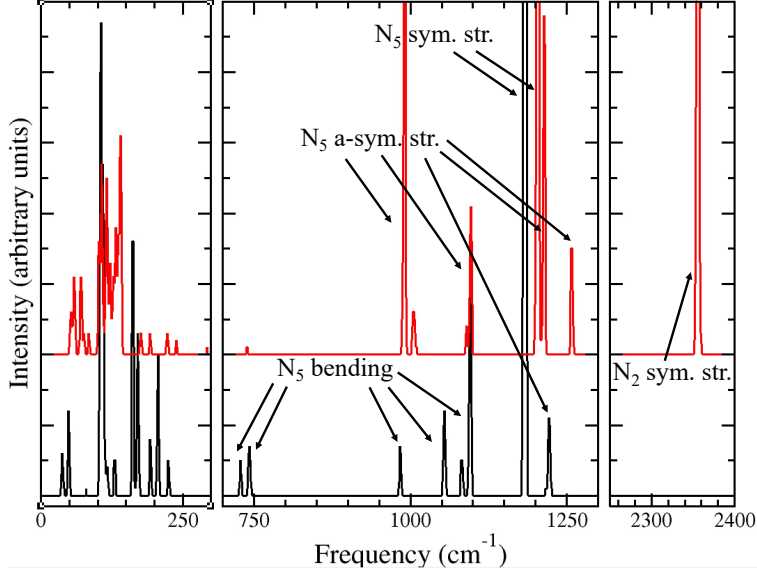


Figure 5: Calculated Raman spectra of $\text{AgN}_5\text{-}P2_1/c$, black curve, and $\text{AgN}_6\text{-}P2_12_12$, red curve, at 0 GPa zoomed to show smaller peaks. The tallest peak of $\text{AgN}_5\text{-}P2_1/c$ at 1183.4 cm^{-1} is nearly 7 times larger than the next tallest peak at $\sim 106\text{ cm}^{-1}$. The tallest peak of $\text{AgN}_6\text{-}P2_12_12$ at 1200.2 cm^{-1} corresponding to the symmetric stretching of the N_5^- molecule is 1.42 times larger than the next tallest peak at 2355.9 cm^{-1} corresponding to the symmetric stretching of the N_2 dimer. The specific bending and stretching modes are labeled in the high frequency range.

A material must be at least dynamically stable at ambient conditions to be considered as a viable candidate for experimental synthesis. The dynamical stability of $\text{AgN}_5\text{-}P2_1/c$ at 0 GPa is confirmed via the absence of negative phonon frequencies in phonon band structure, see Fig. S3 in the supplementary information. To aid in the experimental identification of $\text{AgN}_5\text{-}P2_1/c$, its Raman spectrum is calculated at 0 GPa, see Fig. 5. The lattice and N_5^- librational modes are in the low frequency range of the Raman spectra, i.e. from 37.6 to 225.4 cm^{-1} . There are six bending modes in the Raman spectra: two twisting modes at 728.4 and 742.6 cm^{-1} and four scissoring modes at 984.2 , 1054.8 , 1083 , and 1101.3 cm^{-1} . The most intense peak is the symmetric stretching mode at 1183.4 cm^{-1} while the last mode at 1222 cm^{-1} is an anti-symmetric stretching mode. These results appear to agree well with experimental Raman spectra presented by Sun *et al.*¹⁷. Specifically, both structures show symmetric stretching modes, with the mode reported in this study at 1183.4 cm^{-1} and Sun

et al. reporting theirs at 1187 cm^{-1} .¹⁷ There are also two bending modes reported in each study that are close in frequency, those at 1054.8 and 1101.3 cm^{-1} in this study and at 1020 and 1122 cm^{-1} in Sun *et al.*'s work.¹⁷

Negative phonon frequencies at ambient conditions are also not present in case of $\text{AgN}_6\text{-}P2_12_12$, see Fig. S4 in the supplementary information. The Raman spectra of this crystal are also calculated at 0 GPa to aid in its experimental identification, see Fig. 5. The lattice and N_5^- librational modes are found in the low frequency range of 55.4 to 293.2 cm^{-1} . Unlike $\text{AgN}_5\text{-}P2_1/c$, there are no N_5^- bending modes present in $\text{AgN}_6\text{-}P2_12_12$. The most frequent type of mode is anti-symmetric stretching of the N_5^- molecule with a total of 6 modes at 990.7 , 1005.1 , 1089.7 , 1097.6 , 1214.3 , and 1259.2 cm^{-1} . There are two symmetric stretching modes in the Raman spectra. The mode at 1200.2 cm^{-1} is the symmetric stretching of the N_5^- molecule and the mode at 2355.9 cm^{-1} is the symmetric stretching of the N_2 dimer. In comparing the Raman spectra of $\text{AgN}_5\text{-}P2_1/c$ and $\text{AgN}_6\text{-}P2_12_12$, it can be seen that the crystals possess very different characteristics. The last modes for both $\text{AgN}_5\text{-}P2_1/c$ and $\text{AgN}_6\text{-}P2_12_12$ are anti-symmetric stretching modes but differ in frequency by about 37 cm^{-1} . The most intense peak of both crystals is the symmetric stretching mode found at 1183.4 cm^{-1} for $\text{AgN}_5\text{-}P2_1/c$ and at 1200.2 cm^{-1} for $\text{AgN}_6\text{-}P2_12_12$. $\text{AgN}_6\text{-}P2_12_12$ contains no bending modes compared to the six found in $\text{AgN}_5\text{-}P2_1/c$. Therefore, the correspondence between $\text{AgN}_5\text{-}P2_1/c$ crystal and that synthesized by Sun *et al.*'s¹⁷ can unambiguously rule out the appearance of $\text{AgN}_6\text{-}P2_12_12$ in experiment.

Conclusions

Using first-principles evolutionary structure prediction calculations, we discovered two novel silver pentazolate compounds: $\text{AgN}_5\text{-}P2_1/c$ and $\text{AgN}_6\text{-}P2_12_12$, which are predicted to be thermodynamically stable at pressures 41.5 Pa and 41.7 GPa, respectively. These structures are proved to be dynamically stable at 0 GPa. In contrast to AgN_5 novel pentazolate AgN_6

compound contains N_2 diatomic molecules in addition to cyclo- N_5^- . Synthesis of AgN_5-P2_1/c may be possible by compressing mixture of N_2 and AgN_3 to pressures above 21.42 GPa at which point AgN_5-P2_1/c is becoming thermodynamically favorable. Synthesis of $AgN_6-P2_12_12$ may be possible at pressures above 25.58 GPa via the same route. The Raman spectra of both AgN_5-P2_1/c and $AgN_6-P2_12_12$ are presented. We report agreement between calculated Raman spectrum of and experimental data from Sun *et al.*¹⁷ and is therefore strong evidence that this structure was synthesized in experiment.

Acknowledgement

The research is supported by DOE/NNSA (grant # DE-NA0003910). Computations were performed using leadership-class HPC systems: OLCF Summit at Oak Ridge National Laboratory (ALCC and INCITE awards MAT198) and TACC Frontera at University of Texas at Austin (LRAC award #DMR21006) and USF Research Computing Cluster CIRCE. email: oleynik@usf.edu

Conflict of Interest Statement

The authors declare there are no competing financial interests.

References

- (1) Steinhauser, G.; Klapotke, T. M. *Angewandte Chemie International Edition* **2008**, *47*, 3330–3347.
- (2) Brinck, T. In *Green Energetic Materials*; Brinck, T., Ed.; John Wiley & Sons, Ltd: Chichester, United Kingdom, 2014; pp 1–290.
- (3) Klapotke, T. M. *High Energy Density Materials*; Springer Berlin Heidelberg: Berlin, Heidelberg, 2007; Vol. 125; pp 85–121.

- (4) Zarko, V. E. *Combustion, Explosion, and Shock Waves* **2010**, *46*, 121–131.
- (5) Mailhot, C.; Yang, L. H.; McMahan, A. K. *Physical Review B* **1992**, *46*, 14419–14435.
- (6) Eremets, M. I.; Gavriiliuk, A. G.; Trojan, I. A.; Dzivenko, D. A.; Boehler, R. *Nature Materials* **2004**, *3*, 558–563.
- (7) Tomasino, D.; Kim, M.; Smith, J.; Yoo, C.-S. *Physical Review Letters* **2014**, *113*, 205502.
- (8) Eremets, M. I.; Trojan, I. A.; Gavriiliuk, A. G.; Medvedev, S. A. In *Static Compression of Energetic Materials*; Peiris, S. M., Piermarini, G. J., Eds.; Springer Berlin Heidelberg: Berlin, Heidelberg, 2008; pp 75–97.
- (9) Bazanov, B.; Geiger, U.; Carmieli, R.; Grinstein, D.; Welner, S.; Haas, Y. *Angewandte Chemie International Edition* **2016**, *55*, 13233–13235.
- (10) Steele, B. A.; Oleynik, I. I. *Chemical Physics Letters* **2016**, *643*, 21–26.
- (11) Steele, B. A.; Stavrou, E.; Crowhurst, J. C.; Zaug, J. M.; Prakapenka, V. B.; Oleynik, I. I. *Chemistry of Materials* **2017**, *29*, 735–741.
- (12) Steele, B. A.; Oleynik, I. I. *The Journal of Physical Chemistry A* **2017**, *121*, 1808–1813.
- (13) Williams, A. S.; Steele, B. A.; Oleynik, I. I. *The Journal of Chemical Physics* **2017**, *147*, 234701.
- (14) Xu, Y.; Wang, Q.; Shen, C.; Lin, Q.; Wang, P.; Lu, M. *Nature* **2017**, *549*, 78–81.
- (15) Zhang, C.; Yang, C.; Hu, B.; Yu, C.; Zheng, Z.; Sun, C. *Angewandte Chemie International Edition* **2017**, *56*, 4512–4514.
- (16) Zhang, C.; Sun, C.; Hu, B.; Yu, C.; Lu, M. *Science* **2017**, *355*, 374–376.

- (17) Sun, C.; Zhang, C.; Jiang, C.; Yang, C.; Du, Y.; Zhao, Y.; Hu, B.; Zheng, Z.; Christe, K. O. *Nature Communications* **2018**, *9*, 1269.
- (18) Laniel, D.; Weck, G.; Gaiffe, G.; Garbarino, G.; Loubeyre, P. *The Journal of Physical Chemistry Letters* **2018**, *9*, 1600–1604.
- (19) Steele, B. A.; Oleynik, I. I. *The Journal of Physical Chemistry A* **2017**, *121*, 8955–8961.
- (20) Steele, B. A.; Oleynik, I. I. *Challenges and Advances in Computational Chemistry and Physics*; Springer, 2019; Vol. 28; pp 25–52.
- (21) Shen, Y.; Oganov, A. R.; Qian, G.; Zhang, J.; Dong, H.; Zhu, Q.; Zhou, Z. *Scientific Reports* **2015**, *5*, 14204.
- (22) Peng, F.; Han, Y.; Liu, H.; Yao, Y. *Scientific Reports* **2015**, *5*, 16902.
- (23) Yi, W.; Jiang, X.; Yang, T.; Yang, B.; Liu, Z.; Liu, X. *ACS Omega* **2020**, 24946–24953.
- (24) Zhou, M.; Sui, M.; Shi, X.; Zhao, Z.; Guo, L.; Liu, B.; Liu, R.; Wang, P.; Liu, B. *The Journal of Physical Chemistry C* **2020**, *124*, 11825–11830.
- (25) Bykov, M.; Bykova, E.; Chariton, S.; Prakapenka, V. B.; Batyrev, I. G.; Mahmood, M. F.; Goncharov, A. F. *Dalton Transactions* **2021**, *50*, 7229–7237.
- (26) Lifschitz, J. *Berichte der deutschen chemischen Gesellschaft* **1915**, *48*, 410–420.
- (27) Curtius, T.; Darapsky, A.; Müller, E. *Berichte der deutschen chemischen Gesellschaft* **1915**, *48*, 1614–1634.
- (28) Shanley, E. S.; Ennis, J. L. *Industrial & Engineering Chemistry Research* **1991**, *30*, 2503–2506.
- (29) Guo, G. C.; Wang, Q. M.; Mak, T. C. *Journal of Chemical Crystallography* **1999**, *29*, 561–564.

- (30) Ennis, J. L. *Journal of chemical education* **1991**, *68*, A–6, A–8.
- (31) Kleine, H.; Dewey, J. M.; Ohashi, K.; Mizukaki, T.; Takayama, K. *Shock Waves* **2003**, *13*, 123–138.
- (32) Luchs, J. K. *Photogr. Sci. Eng.* **1966**, *10*, 334–337.
- (33) Gray, P.; Waddington, T. C. *Proceedings of the Royal Society of London. Series A. Mathematical and Physical Sciences* **1956**, *235*, 481–495.
- (34) Yoo, C. S. *MRS Bulletin* **2017**, *42*, 724–728.
- (35) Oganov, A. R.; Glass, C. W. *The Journal of Chemical Physics* **2006**, *124*, 244704.
- (36) Glass, C. W.; Oganov, A. R.; Hansen, N. *Computer Physics Communications* **2006**, *175*, 713–720.
- (37) Lyakhov, A. O.; Oganov, A. R.; Valle, M. *Computer Physics Communications* **2010**, *181*, 1623–1632.
- (38) Pickard, C. J.; Needs, R. J. *Physical Review Letters* **2009**, *102*, 125702.
- (39) Ma, Y.; Oganov, A. R.; Xie, Y. *Physical Review B* **2008**, *78*, 014102.
- (40) Hermann, A. *Reviews in Computational Chemistry*; John Wiley & Sons, Inc., 2017; pp 1–41.
- (41) Perdew, J. P.; Burke, K.; Ernzerhof, M. *Physical Review Letters* **1996**, *77*, 3865–3868.
- (42) Kresse, G.; Furthmüller, J. *Computational Materials Science* **1996**, *6*, 15–50.
- (43) Lazzeri, M.; Mauri, F. *Physical Review Letters* **2003**, *90*, 036401.
- (44) Porezag, D.; Pederson, M. R. *Physical Review B* **1996**, *54*, 7830–7836.
- (45) Manz, T. A.; Sholl, D. S. *Journal of Chemical Theory and Computation* **2010**, *6*, 2455–2468.

- (46) Hou, D.; Zhang, F.; Ji, C.; Hannon, T.; Zhu, H.; Wu, J.; Levitas, V. I.; Ma, Y. *Journal of Applied Physics* **2011**, *110*, 023524.
- (47) Li, D.; Zhu, P.; Wang, Y.; Liu, B.; Jiang, J.; Huang, X.; Wang, X.; Zhu, H.; Cui, Q. *RSC Advances* **2016**, *6*, 82270–82276.
- (48) Zhu, W.; Xiao, H. *Journal of Solid State Chemistry* **2007**, *180*, 3521–3528.
- (49) Erba, A.; Maschio, L.; Pisani, C.; Casassa, S. *Physical Review B* **2011**, *84*, 012101.
- (50) Plasienka, D.; Martonak, R. *The Journal of Chemical Physics* **2015**, *142*, 094505.
- (51) Alkhaldi, H.; Kroll, P. *Journal of Physical Chemistry C* **2019**, 7054–7060.